31st Annual International Conference of the IEEE EMBS
Minneapolis, Minnesota, USA, September 2-6, 2009

Electrotonic effects on action potential duration in perfused rat hearts

Richard D. Walton, and Olivier Bernus

Abstract—**Electrotonic interactions in cardiac tissue have been shown previously to modulate dynamical properties of the myocardium such as action potential duration (APD) and action potential duration restitution. A recent computational study indicated that these electrotonic effects may be strongest in small murine hearts. In the present study, we investigate experimentally how APD is modulated by activation sequence and pacing rate using optical mapping in Langendorff perfused rat hearts. Our results show that following an epicardial point stimulus, a strong correlation exists between epicardial APD and activation time, with decreasing APD for increasing activation time. This effect is preserved for all pacing frequencies (6-14Hz) investigated in this study. Our experimental results are validated by detailed three-dimensional computer simulations. These simulations also demonstrate a strong transmural APD dependence on activation sequence, which, near the pacing site, is sufficient to mask the intrinsic transmural gradient.**

I. Introduction

Heterogeneity in cardiac tissue has been found in both normal and pathological myocardium. Regional variations in action potential duration (APD) are probably one of the best characterized forms of heterogeneity in the heart. Evidence from many species has shown that transmural as well as base-to-apex gradients in APD exist in healthy myocardium[1, 2], largely due to varying levels of repolarizing ionic current expressions (e.g. [3]). Although such regional differences are believed to be important in the normal functioning of the heart, it is also known that enhanced APD dispersion in disease can provide a mechanism for conduction blocks and arrhythmogenesis [4].

APD heterogeneity is in part determined by the intrinsic properties of the myocardial cells, but it has also been shown to depend on cell-to-cell coupling and activation pattern [5-9]. Electrotonic interactions due to the coupling of cells in tissue are capable of gradually decreasing the duration of an action potential as it propagates away from the pacing site, with the strongest effect found in the direction of small conduction velocities [9], or for reduced coupling [6]. Cell-to-cell coupling has also been found to modulate the rate-dependency of APD, i.e. APD restitution [6, 8]. Since the steepness of APD restitution curves has been implicated in arrhythmogenesis, it is important to understand which factors can modulate this dynamical property of cardiac tissue.

A recent computational study in isotropic whole hearts indicated that electrotonic effects could completely mask the intrinsic APD heterogeneity in small murine hearts [5]. This study showed that the transmembrane resistance during recovery determined by the transmembrane ionic currents plays a major role in the electrotonic APD modulation; this effect being more pronounced for murine action potentials than for rabbit action potentials. However, the role of pacing frequency and anisotropic conduction in murine hearts commonly used in experimental study remains unclear.

The goal of this project was therefore to investigate experimentally the electrotonic modulation of APD in Langendorff perfused rat hearts using optical mapping. Our results indicate that following epicardial point stimulation there is a strong correlation between activation time and APD, thus indicating the important role of electrotonic currents. This effect is preserved for a wide range of pacing frequencies. Computer simulations confirm our findings and also indicate that electrotonic effects on APD could have profound implications on the transmural APD gradient.

II. Methods

A. Langendorff perfused rat hearts

Male Wistar rats (N = 5) were killed in accordance with the Animals (Scientific Procedures) Act 1986. Hearts were rapidly removed and arrested in ice cold cardioplegic solution containing (in mM): glucose, 277.5; KCl, 30; NaHCO3, 25; mannitol, 34.3, pH 7.4. The aorta was cannulated and perfused at 7 ml/min with bicarbonate buffered saline solution containing (mM): NaCl, 130; NaHCO3, 24; NaH2PO4, 1.2; MgCl2, 1; glucose, 5.6; KCl, 4; CaCl2; oxygenated with 95% O2/5% CO2, pH 7.4, 37 °C. 10 μM blebbistatin was added to stop contraction [10]. The tissue was stained with potentiometric dye Di-4-ANEPPS (5 μg/ml normal Tyrode's solution) via the perfusate at the beginning of the experiment. Bipolar electrodes were used to stimulate the ventricles at the epicardial surface at cycle lengths ranging from 165 - 70 ms. A dynamic pacing protocol was used whereby hearts were allowed to stabilize at each pacing frequency (minimum 10 s) prior to recording.

B. Optical Mapping

Optical recordings were acquired through a high-frame-rate charge-coupled device video camera (SciMeasure Analytical systems, GA, USA) mounted with a lens (focal length 12 mm, 1:0.8 aperture ratio; Computar, London, UK).

Manuscript received April 23, 2009. This work was supported in part by the Engineering and Physical Sciences Research Council (EP/F065574/1) and the Royal Society (RG081248).

R.D. Walton and O. Bernus are with the Multidisciplinary Cardiovascular Research Centre and the Institute of Membrane and Systems Biology at the University of Leeds (phone: +44-113-343-4235; fax: +44-113-343-4228; e-mail: o.bernus@leeds.ac.uk).

Excitation light from a monochromatic laser, 532 nm, (Shanghai Dreamlasers technology Co., Ltd, Shanghai, China) was passed through a beam expander to illuminate the epicardial surface. Emission light was filtered through broadband 700DF50 filters. Images (80 x 80 pixels) with pixel dimensions of 0.25 x 0.25 mm were acquired at a rate of 2000 frames per second. Background fluorescence was subtracted from each frame to obtain the voltage-dependent optical signal.

In all experiments, optical action potentials (OAP) recorded over 5 s underwent temporal (3 ms kernel) and spatial (1.25 mm kernel) filtration followed by ensemble averaging. Activation times were measured at a level of 50% of the optical/electrical AP upstroke. Action potential duration (APD) was measured at a level of 80% of repolarisation. Pixel values for APD were plotted against activation times acquired from corresponding pixels. Data for APD at 80%, 50% and 25% repolarisation were acquired from 49 pixels in different locations and statistical differences were determined using a Student's T-test.

C. *Computer simulations*

Optical signals of cardiac electrical activity are simulated using a photon transport model coupled to a rat electrophysiological model [11]. We used the diffusion equation with partial-flux boundary conditions for the photon transport model, as it was previously shown to be sufficiently accurate in reproducing the effects of scattering on action potential upstrokes [12].

Electrical activity was simulated using a reaction-diffusion equation and with conduction velocities of 60 cm/s in longitudinal and 20 cm/s in transverse directions of fiber orientation as in previous studies [12]. Fiber orientation was assumed to rotate transmurally at a fixed rate of 40°/mm. Propagation of electrical waves was simulated in rectangular slabs of 10 mm x 10 mm x 3mm. A transmural gradient in Ito conductance was implemented from epi- (100%) to endocardium (46%) similar to Pandit et al [11]. This resulted in an intrinsic APD difference between epi- and endocardium of 34 ms. Temporal and spatial resolutions for each simulation were 1 ms and 0.1 mm, respectively.

III. RESULTS

A. *APD vs. activation time*

The electrotonic effects on APD in rat hearts were investigated for two different pacing locations: (i) the anterior insertion site of the left ventricle with the septum, and (ii) the LV mid-free wall. Fig. 1 shows the results for the anterior pacing location both for computation and a representative experiment when pacing at 6Hz. Panel (a) shows epicardial activation time and APD maps, whereas panel (b) shows the corresponding experimental maps. Anisotropic propagation manifested by the ellipsoidal shape of the wave front can be observed in both simulation and experiments. APD is longest near the pacing site (65 ms and 64 ms for simulation and experiment respectively) and gradually decreases with increasing distance from the stimulation site. This decrease is the most pronounced in the direction of slow propagation, and indicates a correlation between APD and activation time.

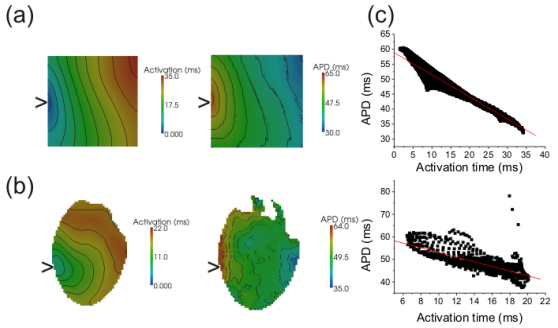

Fig. 1. Correlation between OAP activation times and APD for anterior pacing (arrow). (a) Activation map (left panel) and APD map (right panel) derived from a hybrid optical-electrical simulation. Isochrones and isobars are at 3 ms intervals for activation and APD maps, respectively. (b) Activation map (left panel) and APD map (right panel) derived from experiments. Isochrones and isobars are at 2 ms intervals for activation and APD maps, respectively. (c) APD and activation time plots for simulation (upper panel) and experiments (lower panel).

Linear regression analysis was therefore performed between APD and activation time in each pixel of the imaged surface and the results are presented in panel (c). The top graph shows a strong linear correlation for the simulated optical signals (R=0.99). The red line represents the linear fit to the data. The bottom graph shows the corresponding plot for the experimental data. Although the result is more dispersed, a strong correlation between APD and activation time can still be observed (R=0.86).

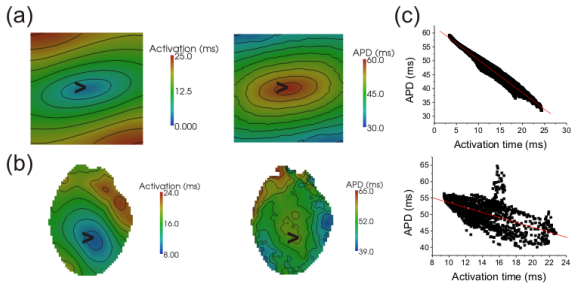

Fig. 2. Correlation between OAP activation times and APD for mid-free wall pacing (arrow). (a) Activation map (left panel) and APD map (right panel) derived from a hybrid optical-electrical simulation. Isochrones and isobars are at 3 ms intervals for activation and APD maps, respectively. (b) Activation map (left panel) and APD map (right panel) derived from experiments. Isochrones and isobars are at 2 ms intervals for activation and APD maps, respectively. (c) APD and activation time plots for simulation (upper panel) and experiments (lower panel).

Fig. 2 shows the results for the LV mid-free wall 6Hz pacing in the same heart as in Fig. 1. The location of maximal APD is again at the pacing location, clearly indicating the electrotonic modulation of APD in these hearts. Again, we observe a gradual decrease of APD for increasing distance with respect to the stimulation site, and this effect is strongest in the direction of slow propagation, both in simulation (a) and experiment (b). Linear regression analysis shows here a strong correlation between APD and

activation time as well (R=0.99 and R=0.76 for computation and experiment respectively). Interestingly, in the experiment, the correlation seems to be weaker in the anterior basal region of the heart, with larger APDs at intermediate activation time (see panels (b) and (c)).

B. *APD restitution*

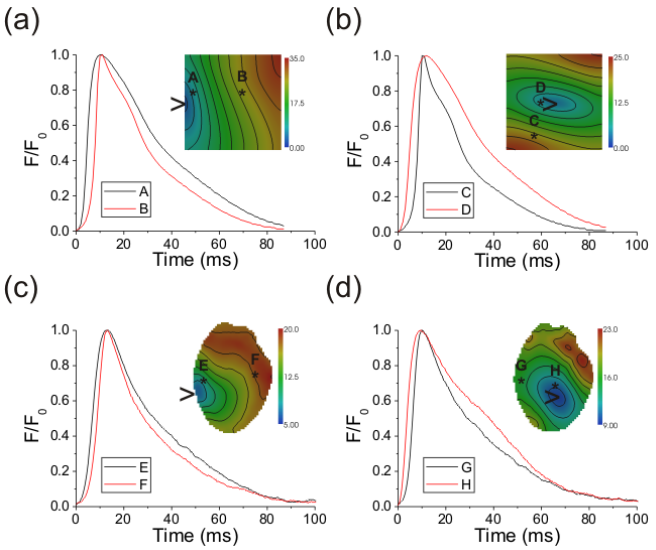

Fig. 3. OAPs recorded from early and late activation times. OAPs were recorded from simulations in the epicardial plane showing point stimulation (arrows) from lateral (a) and medial (b) locations as shown in inserts. Experimental validation was achieved from point stimulation (arrows) at anterior (c) and mid-free wall locations (d) as shown in inserts. Inserts show activation maps indicating pixels (*) for which OAPs were plotted.

Fig. 3 shows optical action potentials recorded from various regions of the heart and for the two different pacing locations. Panels (a) and (b) illustrate simulated OAPs close to and far away from the pacing location, for anterior and mid-free wall pacing respectively. Panels (c) and (d) show the corresponding experimental OAPs. Action potentials were superimposed following subtraction of activation times.

First, all panels indicate that the shape of the optical depolarization phase, i.e. the optical upstroke, depends on the position relative to the pacing location. This is consistent with previous studies that have shown that the shape of the optical upstroke correlates to the sub-surface wave front orientation (e.g. [12]). More relevant to the current study, is the net increase in repolarization rate for sites further away from the pacing location. The OAP traces also clearly demonstrate that the electrotonic APD modulation is present at all repolarization levels, as further illustrated by the data presented in Table 1.

We also investigated the effects of pacing frequency on the electrotonic modulation of APD in our experiments. The results are presented in Fig. 4 for the two pacing locations: anterior in panel (a) and mid-free wall in panel (b). The pacing frequency was gradually increased from 6 Hz to 14 Hz and several minutes were allowed at each frequency for the heart to reach steady-state. APD values were acquired as described in the Methods section from areas shown in inserts (white rectangles). All restitution curves showed a biphasic APD dependency to pacing cycle length, with an increase in APD at shorter pacing cycle lengths. APD was consistently smaller in regions of late activation time at all pacing frequencies. Moreover, in the case of mid-free wall pacing changes in the shape of the restitution curve were observed when comparing regions of early vs. late activation time.

TABLE I
APD AT VARIOUS REPOLARIZATION LEVELS FOR THE TWO PACING LOCATIONS (MEAN ± STANDARD DEVIATION, N = 49 PIXELS, * P<0.0001 COMPARING EARLY *VS.* LATE ACTIVATION TIME)

	APD80 (ms)	APD50 (ms)	APD25 (ms)
Anterior pacing Early activation	52.7 ± 2.8	24.6 ± 1.7	12.3 ± 1.2
Anterior pacing Late activation	47.6 ± 0.5*	22.4 ± 0.3*	10.1 ± 0.3*
Mid-free wall pacing Early activation	55.2 ± 0.4	33.6 ± 0.5	15.5 ± 0.3
Mid-free wall pacing Late activation	50.6 ± 0.9*	23.3 ± 1.8*	10.9 ± 0.6*

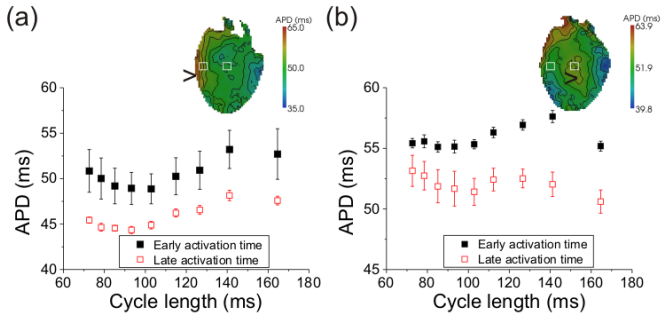

Fig. 4. APD restitution at early and late activation times. APD maps (insert) were from representative experiments with point stimulation (arrows) from anterior (a) and mid-free wall locations (b) at 6Hz.

C. *Electrotonic influences on transmural APD dispersion*

The transmural extent of electrotonic effects was assessed using the computational model since optical recordings are limited to the epicardial surface. Fig. 5 shows activation time (a) and APD (b) maps in a transmural cross section of the simulated rat LV slab, following epicardial point stimulation (pacing frequency = 5 Hz). Note that an intrinsic epi-endo APD gradient was modeled in this slab (see Methods). The transmural fiber rotation leads to the typical activation pattern observed in panel (a). The APD map shown in panel (b) indicates strong electrotonic effects here as well: the transmural APD gradient measured right under the pacing site is largely reduced (5 ms maximal dispersion). Further away from the pacing site, larger transmural gradients are observed, but with overall smaller APD values, as illustrated in panel (c).

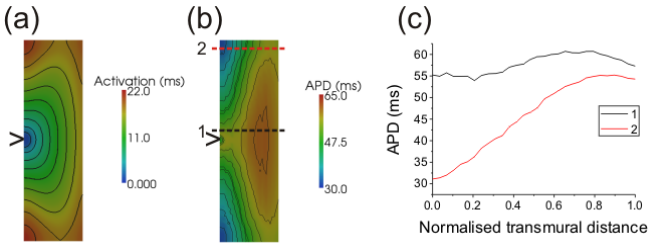

Fig. 5. Transmural dispersion of APD following epicardial stimulation (arrow). (a) Activation map of electrical propagation where isochrones are at 3 ms intervals. (b) Corresponding APD map where isobars are at 3 ms intervals. (c) Transmural profiles of APD taken from regions associated with early (1) and late (2) epicardial activation times, as indicated.

IV. Discussion

The goal of the present study was to characterize the effects of electrotonic currents on APD dispersion in Langendorff perfused rat hearts. Our main conclusion is that there exists a strong electrotonic modulation of APD on the rat left ventricular epicardium as shown by our optical mapping recordings, which were further validated using a detailed computational model (see Fig. 1 and 2). Our experimental results indicate that cell-to-cell coupling can almost completely mask intrinsic heterogeneities on the epicardial surface of these hearts, thus validating earlier computational work. It is worth noting that in some experiments, the anterior basal region would display long action potentials whose duration would only be slightly modulated by pacing location and activation pattern (compare panels (b) in Figs. 1 and 2). This may be due to an intrinsically much longer APD in those regions, which would require further investigation. Nevertheless, we found in all experiments and simulations, and for two different pacing locations, a strong correlation between APD and activation time.

Electrotonic interactions between cells have previously been shown to modulate the APD rate-dependency, especially at short cycle lengths, and hence to change the steepness of the APD restitution curve [6, 8]. This resulted in increased APD dispersion at high pacing frequencies or short coupling intervals. These studies have been performed in animal species or computational models that display positively sloped restitution curves. However, rat tissue is known to display negatively sloped restitution, due to different expressions of transmembrane ionic currents when compared to larger mammalian species [13]. In our experiments, we also observed negatively sloped restitution curves. Here, APD was always shorter at later activation times, independent of pacing frequency. Although in most recordings the APD dispersion did not increase with increasing pacing frequency (e.g. Fig. 4a), we did observe decreased APD dispersion at shorter cycle length in some experiments (e.g. in Fig. 4b). This observation could be the result of the distinct murine electrophysiology, but will require a more careful analysis.

Cardiac epi-fluorescence imaging using dyes such as DI-4-ANEPPS provides information about a relatively shallow sub-epicardial layer. However, electrotonic APD modulation should also be present transmurally [5]. The three-dimensional computational model used in this study indicates that this is indeed the case (Fig. 5): we found that near the stimulation site the transmural APD gradient was significantly reduced with only little difference between the epicardial and endocardial APDs (profile 1 in Fig. 5c). Further away from the pacing location (profile 2 in Fig. 5c), a transmural gradient is recovered, with longer APDs near the endocardium. However, even at the endocardium the APD is shorter here than right under the stimulating electrode, consistent with the larger activation time.

References

[1] C. Antzelevitch, "Modulation of transmural repolarization," Ann N Y Acad Sci, vol. 1047, pp. 314-23, Jun 2005.

[2] X. Wan, S. M. Bryant, and G. Hart, "A topographical study of mechanical and electrical properties of single myocytes isolated from normal guinea-pig ventricular muscle," J Anat, vol. 202, pp. 525-36, Jun 2003.

[3] S. P. Patel and D. L. Campbell, "Transient outward potassium current, 'Ito', phenotypes in the mammalian left ventricle: underlying molecular, cellular and biophysical mechanisms," J Physiol, vol. 569, pp. 7-39, Nov 15 2005.

[4] C. Antzelevitch, "Role of spatial dispersion of repolarization in inherited and acquired sudden cardiac death syndromes," Am J Physiol Heart Circ Physiol, vol. 293, pp. H2024-38, Oct 2007.

[5] K. J. Sampson and C. S. Henriquez, "Electrotonic influences on action potential duration dispersion in small hearts: a simulation study," Am J Physiol Heart Circ Physiol, vol. 289, pp. H350-60, Jul 2005.

[6] Z. Qu, "Dynamical effects of diffusive cell coupling on cardiac excitation and propagation: a simulation study," Am J Physiol Heart Circ Physiol, vol. 287, pp. H2803-12, Dec 2004.

[7] C. E. Conrath, R. Wilders, R. Coronel, J. M. De Bakker, P. Taggart, J. R. De Groot, and T. Opthof, "Intercellular coupling through gap junctions masks M cells in the human heart," Cardiovasc Res, vol. 62, pp. 407-14, May 1 2004.

[8] K. R. Laurita, S. D. Girouard, Y. Rudy, and D. S. Rosenbaum, "Role of passive electrical properties during action potential restitution in intact heart," Am J Physiol, vol. 273, pp. H1205-14, Sep 1997.

[9] T. Osaka, I. Kodama, N. Tsuboi, J. Toyama, and K. Yamada, "Effects of activation sequence and anisotropic cellular geometry on the repolarization phase of action potential of dog ventricular muscles," Circulation, vol. 76, pp. 226-36, Jul 1987.

[10] V. V. Fedorov, I. T. Lozinsky, E. A. Sosunov, E. P. Anyukhovsky, M. R. Rosen, C. W. Balke, and I. R. Efimov, "Application of blebbistatin as an excitation-contraction uncoupler for electrophysiologic study of rat and rabbit hearts," Heart Rhythm, vol. 4, pp. 619-26, May 2007.

[11] S. V. Pandit, R. B. Clark, W. R. Giles, and S. S. Demir, "A mathematical model of action potential heterogeneity in adult rat left ventricular myocytes," Biophys J, vol. 81, pp. 3029-51, Dec 2001.

[12] C. J. Hyatt, C. W. Zemlin, R. M. Smith, A. Matiukas, A. M. Pertsov, and O. Bernus, "Reconstructing subsurface electrical wave orientation from cardiac epi-fluorescence recordings: Monte Carlo versus diffusion approximation," Opt Express, vol. 16, pp. 13758-72, Sep 1 2008.

[13] L. Salle, S. Kharche, H. Zhang, and F. Brette, "Mechanisms underlying adaptation of action potential duration by pacing rate in rat myocytes," Prog Biophys Mol Biol, vol. 96, pp. 305-20, Jan-Apr 2008.